Max-Planck-Institut
für Meteorologie

REPORT No. 71

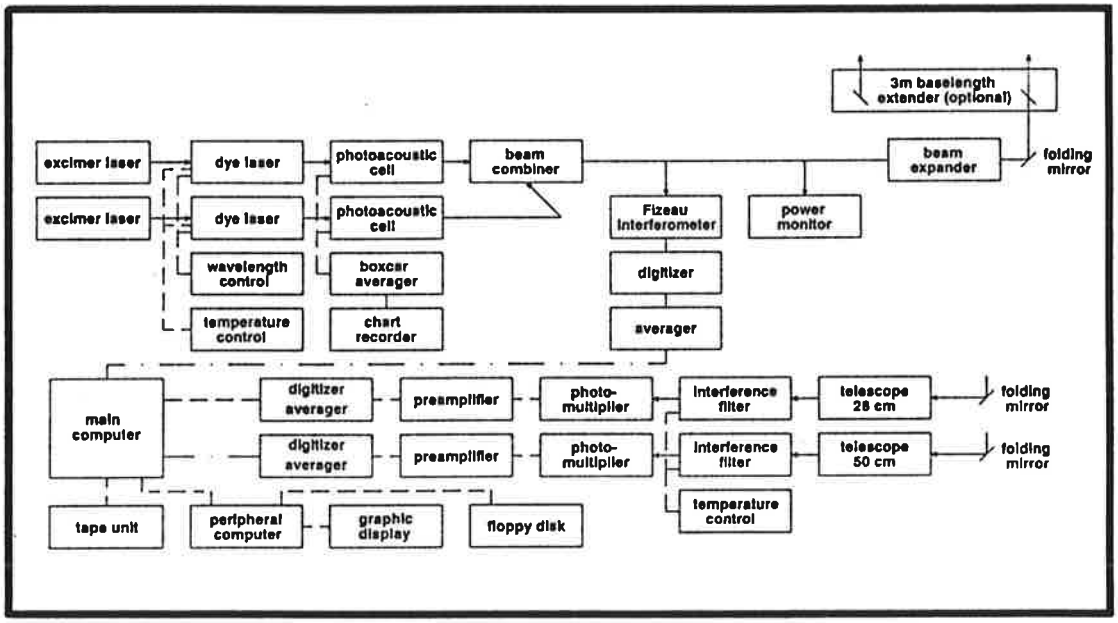

A DIFFERENTIAL ABSORPTION LIDAR SYSTEM FOR HIGH RESOLUTION WATER VAPOR MEASUREMENTS IN THE TROPOSPHERE

by

JENS BÖSENBERG

HAMBURG, SEPTEMBER 1991

AUTHOR:

JENS BÖSENBERG

MAX-PLANCK-INSTITUT
FUER METEOROLOGIE

MAX-PLANCK-INSTITUT
FUER METEOROLOGIE
BUNDESSTRASSE 55
D-2000 HAMBURG 13
F.R. GERMANY

Tel.: +49 (40) 4 11 73-0
Telex: 211092 mpime d
Telemail: MPI.METEOROLOGY
Telefax: +49 (40) 4 11 73-298

REPb71

A differential absorption lidar system for high resolution water vapor measurements in the troposphere

Jens Bösenberg
Max-Planck-Institut für Meteorologie
Bundesstr. 55, D-2000 Hamburg 13

September 1991

ISSN 0937–1060

Abstract

A differential absorption lidar system is described using 2 Excimer pumped dye lasers as transmitters. The system is suitable for high resolution measurements in the planetary boundary layer as well as for measurements with reduced resolution in the upper troposphere. The methodology is explained, the sources of errors are discussed, test methods are described, and measurements are presented for the boundary layer as well as for the upper troposphere, clearly demonstrating the capabilities of the system for investigations of meteorological processes.

1 Introduction

Water vapor is one of the most important constituents of the atmosphere:

- the hydrological cycle is very important for life on earth
- it is the most abundant greenhouse gas
- it determines the formation of clouds, which in turn control a large portion of the radiation budget
- it plays a major role in many atmospheric processes

For an improved understanding of these processes detailed information on the moisture field and its variation in space and time on largely varying scales is very important. Conventional in situ measurements often cannot provide sufficient information. Therefore, remote sensing instruments have been developed. If we restrict ourselves to instruments with rather high temporal and spatial resolution, only active optical methods (i.e. Lidar methods) are adequate. So far two methods have been investigated in detail, namely Differential Absorption Lidar (DIAL), and Raman scattering Lidar. Both methods are fairly complicated, so there is no "obvious" choice from the beginning, and the best choice may even depend on the particular application.

The DIAL technique has been investigated using wavelengths in the near infrared around $725nm$ [1, 2, 3, 4, 5], and in the $10\mu m$ region with CO_2 - lasers using both direct detection [6, 7, 8] and heterodyne detection methods [9, 10]. There are major differences between the CO_2 - laser systems

and those operating in the NIR, which are mainly due to the different laser technology (discrete emission lines versus continuous tunability; pulse length of $0.3 - 2\mu sec$ versus pulse length $< 20nsec$). Different scattering mechanisms, aerosol scattering only versus a mixture of aerosol and molecular scattering, also contribute to the different system properties. It is beyond the scope of this paper to evaluate these differences in detail. The Raman scattering technique mostly has been restricted to nighttime measurements [11, 12, 13, 14, 15, 17]. Using a sufficiently short wavelength for excitation so that the Raman signal is in the solar blind region ($\lambda < 295nm$) allows daytime measurements, too [16, 18, 19]. Here some problems arise with absorption by ozone and other pollutants, and aerosol extinction, which have not yet been solved completely. These daytime measurements have been restricted to a range $< 1.5km$, spatial resolution can be quite high, e.g. $5m$ vertical resolution within 2.5 min have been reported [18]. A more complete review of DIAL and Raman measurements of water vapor profiles may be found in reference [20].

When the development of the present system was started, the request was for a versatile instrument with capabilities to resolve rather small scale convective structures in the lower troposhere ($\approx 100m$ vertical and $\approx 30sec$ temporal resolution), as well as measurements in the upper troposphere, e.g. at cirrus level ($\approx 10km$). Daytime operation was deemed necessary, and an accuracy of $5 - 10\%$ was requested. With these needs, only a DIAL system was expected to satisfy the demands. This paper will show, how these requirements are met with the present system.

2 Methodology

2.1 Basic principles

The principles of the DIAL technique have often been described, see e.g. [21], and may briefly be summarized as follows. The range resolved return signal produced by a short laser pulse transmitted into the atmosphere for a monostatic configuration (transmitter and receiver collocated) is described by the Lidar equation

$$P_i(R) = \frac{P_0 \cdot E \cdot F}{R^2} \cdot \beta_i(R) \cdot e^{-2\int_0^R (\alpha_i(r)+\gamma_i(r))dr} \qquad (1)$$

where P_i is the received signal from range R, P_o is transmitted power, E is system efficiency (optical system plus detector), F is receiver area, $\beta_i(R)$ is backscatter coefficient, $\gamma_i(R)$ is extinction coefficient except for the absorption coefficient $\alpha_i(R)$ of the gas under study. If one adds another measurement at a slightly different wavelength indicated by a different subscript i in the Lidar equation, a simple solution for $\alpha_1(R) - \alpha_2(R)$ may be found provided that $\beta_1(R) = \beta_2(R)$ and $\gamma_1(R) = \gamma_2(R)$, namely the DIAL equation

$$\begin{aligned} n(\overline{R}) \cdot (\sigma_1(\overline{R}) - \sigma_2(\overline{R})) &= \alpha_1(\overline{R}) - \alpha_2(\overline{R}) \\ &= -\frac{1}{2 \cdot (R_2 - R_1)} \cdot \ln \frac{P_1(R_2) \cdot P_2(R_1)}{P_2(R_2) \cdot P_1(R_1)} \end{aligned} \quad (2)$$

where the absorption coefficient α is expressed as a product of number density $n(R)$ and absorption cross section σ, n and σ are assumed to be constant in the height interval $R_1 \ldots R_2$. The conditions, under which the assumptions about the backscatter- and extinction coefficients at both wavelengths hold have been discussed [21], generally the wavelength intervall has to be small compared to the spectral structures in the backscatter and extinction coefficients, and the time difference between the 2 measurements has to be smaller than the correlation time of the aerosol. The first condition is not critical for near infrared water vapor DIAL, the absorption lines are narrow ($\approx$ 10 pm FWHM at standard pressure and temperature), so a sufficiently small wavelength difference may be selected (we have chosen 50 pm for our measurements). The correlation time of aerosol backscatter averaged over a small scattering volume only can be quite small under certain meteorological conditions (levels with highly variable aerosol content are often found at the upper edge of the boundary layer, for example). To obtain reliable measurements even under these conditions, which are of particular interest in studies of convective processes, a safe estimate for the maximum time difference is a value much smaller than the time needed for a complete exchange of the aerosol found in the scattering volume. Assuming as worst case conditions a beam diameter of $0.1m$ and a windspeed of $30m/sec$, $3msec$ is a lower limit for this exchange time. It is quite clear, that this cannot be achieved by mechanical switching of the wavelength in a single laser. We have chosen a dual laser system instead, with synchronized triggering $200\mu sec$ apart, so the time dependence of the backscatter coefficient cannot cause any problems.

2.2 Influence of the spectral distribution

The Lidar equation used above is valid for monochromatic light only. For actual conditions the finite linewidth of the high power pulsed laser used has to be considered. This has been done by integrating the Lidar equation over the spectral distribution of the transmitted light [22, 23, 24, 25]. It has been pointed out in the abovementioned papers that this leads to a more complex set of equations which cannot be solved simply in the form of a DIAL equation, but an iterative procedure has to be applied instead. Although this is true in principle, a detailed analysis of the individual terms assuming typical measurement conditions shows, that the DIAL equation remains approximately valid for these cases [25, 26, 27]. It should be emphasized,however,that this holds only if, roughly speaking, the bandwidth of the laser is small compared to the width of the absorption line, and if both the total optical depth up to the measurement range and the difference in optical depth between R_2 and R_1 are sufficiently small. Since the corrections for finite bandwidth are only small under these conditions, an approximate knowledge of this bandwidth is sufficient.

The situation is further complicated by the fact, that generally 2 different scattering processes may contribute significantly to the signal strength, namely aerosol and molecular scattering. The first may be considered elastic, i.e. changes in the spectral distribution caused by the scattering process are small compared to the linewidths involved, but the latter produces spectral broadening of the backscattered light mainly by Doppler shift caused by thermal velocities of the molecules. The error caused by this effect generally is small in a homogeneous atmosphere [28], but can be very large where steep gradients are present in the ratio of aerosol to molecular backscatter. A detailed discussion and a correction procedure using the information about the backscatter profile contained in the off line signal may be found in reference [27].

Yet another complication introduced by the spectral distribution found in real world systems is spectral impurity, defined as total energy out of the assumed lineshape for the laser. In a broadly tunable dye laser (width of the gain curve $> 30nm$ typically) consisting of an oscillator and two or more amplifiers amplified spontaneous emission (ASE) is almost unavoidable. Usually it consists of broad band radiation with very low spectral density, and therefore is very hard to determine. To estimate its influence on the

accuracy of a DIAL measurement, assume that the total intensity of the laser P_0 may be split into its relative contributions of the narrowband and broadband radiation according to $P_0 = P_0 \cdot (P_l + P_b)$ where the spectral distribution of P_l is a narrow line of arbitrary but known shape, centered at the water vapor absorption line, from which in the usual way an effective absorption cross section may be calculated, and P_b is broadband emission with absorption cross section ≈ 0. Then the observed optical depth τ_{eff} is given in terms of τ_0, the optical depth for zero spectral impurity, by

$$\tau_{eff} = -\ln\left[P_b + (1 - P_b) \cdot e^{-\tau_0}\right] \tag{3}$$

An absorption coefficient $\alpha' = \frac{d\tau_{eff}}{dz}$ will be determined instead of $\alpha = \frac{d\tau_0}{dz}$, which leads to a relative error

$$\begin{aligned} \frac{\alpha - \alpha'}{\alpha} &= 1 - \frac{d\tau_{eff}}{d\tau_0} \\ &= \frac{P_b}{P_b + (1 - P_b) \cdot e^{-\tau_0}} \end{aligned} \tag{4}$$

which is illustrated in fig.1 for several values of P_b, the relative intensity of the broadband emission. It is obvious, that even small amounts of spectral impurity will cause large errors at sufficient optical depth. So the range of optical depths for which reliable DIAL measurements are possible is clearly restricted by the spectral impurity of the transmitted laser pulse. This range cannot be considerably expanded by correction of this effect, which in principle of cause is possible. The correction will depend very critically on the exact amount of spectral impurity assumed, which in turn is very hard to determine. As already mentioned, the spectral density usually is very low, many orders of magnitude less than in the central line, so for a direct measurement with spectroscopic instruments a very high straylight rejection would be required as well as linearity of the detector circuit over many orders of magnitude. So we did not actually attempt to determine the spectral impurity in this way, our test method will be given below.

It shall suffice here to just mention that the absorption cross section at the center of an absorption line is pressure and temperature dependent. Temperature sensitivity can be minimized by proper choice of the absorption line, there are several suitable lines available with different line strengths as necessary for different meteorological situations [29]. No major changes have

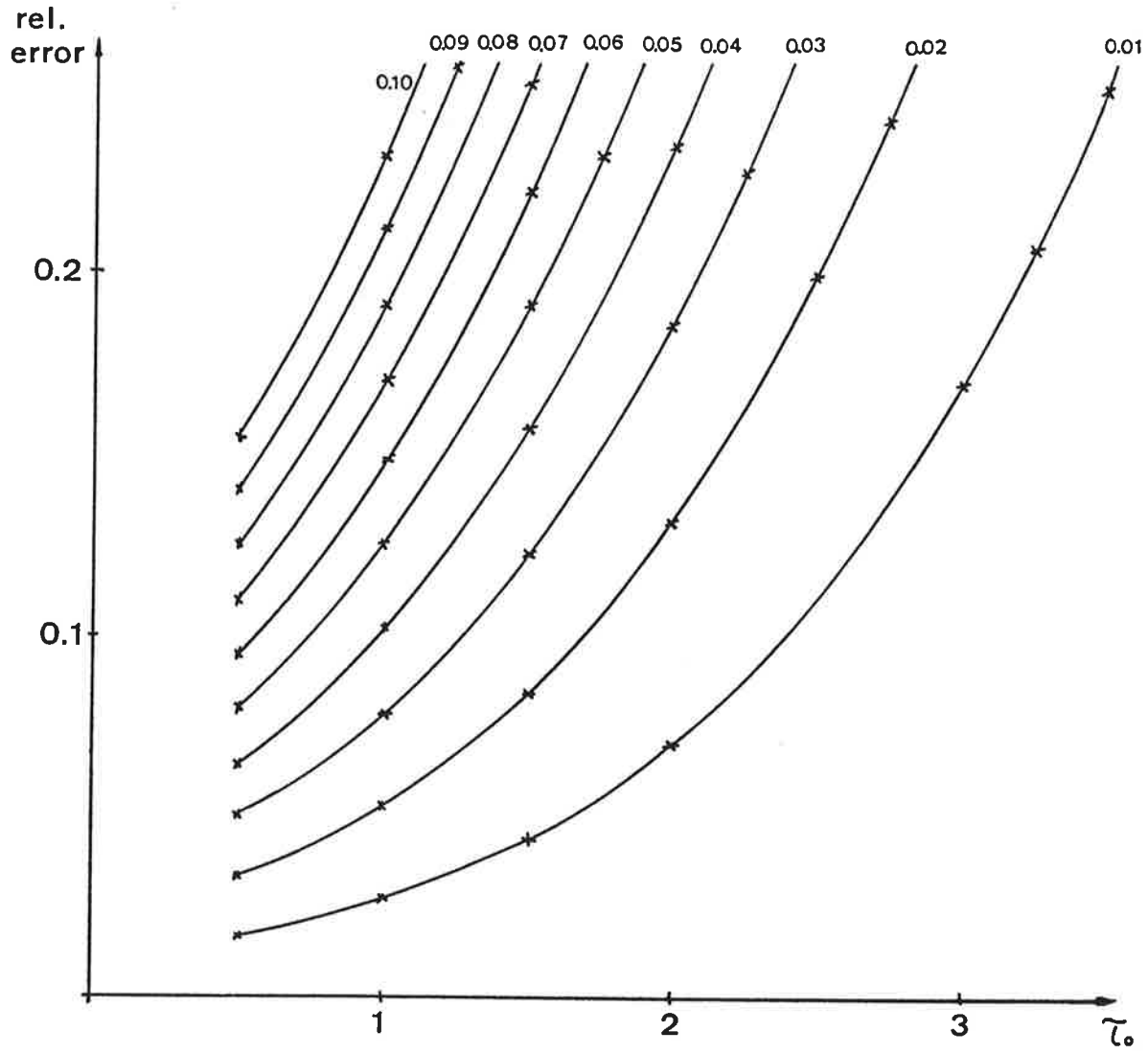

Fig. 1 Relative error of a DIAL measurement due to spectral impurity as a function of optical depth τ_0

to be made in the laser system to access all these lines. Assuming that the temperature dependence of the absorption cross section is governed by the line strength and the Voigt line shape, it is easy to show, that large errors in the atmospheric parameters can be tolerated without sacrificing the accuracy of the measurement. 20 K or 15 hPa error in temperature or pressure, respectively, cause $< 5\%$ error in water vapor concentration throughout the troposphere. So the necessary information on the atmospheric parameters may easily be obtained from routine observations of the weather service at some station in the vicinity.

Pressure shift of the absorption line center has to be considered, too. For most lines this is no problem, when the laser is tuned to the center of the low pressure line. The error produced at surface pressure then usually is negligible, for the line with the largest observed pressure shift [30] it is 10%. Nevertheless, when a new line is considered for a DIAL measurement, for which the pressure shift coefficient has not been determined, it would be good practice to perform such a determination before using this line.

2.3 Data acquisition requirements

The DIAL technique, as a differential method with respect to both wavelength and range, requires high accuracy data acquisition for the individual signals. To give a typical example, assume that a difference in optical depth of 0.1 with a precision of 5% is to be retrieved. Then the error in the individual return signals at range R_1 as well as R_2 must not be greater than 0.25% assuming the best case of statistically independent errors. For a 12 bit digitizer an error in the least significant bit (LSB) corresponds to 0.025%, so a dynamic range of < 10 is left for the signals, which often is exceeded in a rather small height interval. Sometimes it is assumed, that averaging over a large number n of samples can improve the accuracy by a factor of $\sqrt{n}$. While this should hold for the statistical error at least in the case of correlated shot pairs, it is certainly not true for the systematic errors introduced by the digitizer. In fact no manufacturer will specify an equal spacing of digitizer bins, at best monotonicity of the bins is claimed. Test measurements with our system showed, that an accuracy better than 0.2 LSB cannot be assumed, regardless of the number of samples averaged. This restricts the usable dynamic range for the signals to < 50, whereby in turn the usable height range is restricted. Fortunately a sufficiently large portion of the boundary layer

is usually covered, or alternatively a large portion of the upper troposphere, but care has to be taken in the adjustment of the individual signal levels, requiring readjustment in changing meteorological conditions.

3 System description

3.1 Instrument platform

Our system was intended for studies of a variety of meteorological processes. So provisions had to be made to make it transportable to the actual field sites of the individual experiments, which have to be chosen according to the requirements imposed by the process under study. We have restricted ourselves to studies where the site can be fixed for a whole campaign to avoid additional problems caused by true platform mobility. So we have chosen a standard 20' container as a platform which can easily be moved by standard equipment. Insulating walls, a heating and a cooling system provide for an acceptable environment for the delicate instruments and their operators even under rough climatic conditions. A 6 kW cooling system for the lasers is installed separately outside the container. The available space inside measures $5.80 \times 2.19 \times 2.30m$, most of which is occupied by a large rigid frame constructed from aluminum X-profiles. This is mounted vibration isolated during transport and fixed during the measurements, the lasers and optical systems are securely mounted on this frame. The electronics and computer equipment is housed in two 19" racks, only little space is left for the operators. The whole optical system including the 2 telescopes is mounted horizontally, access to the atmosphere is provided by a $1.00 \times 0.70m$ hole in the side wall. Since all measurements are made with a vertically pointing beam, 45° folding mirrors are mounted to a rigid frame in front of the hole. This frame can easily be brought into an upright position, then the mirrors are protected from rain and dirt and the opening in the wall is closed.

3.2 Optical system

An overview over the complete system is given in fig. 2. The laser system consists of 2 XeCl Excimer lasers (Lambda Physik EMG 201 MSC) pumping 2 dye lasers (Lambda Physik FL2002E), each consisting of an oscillator

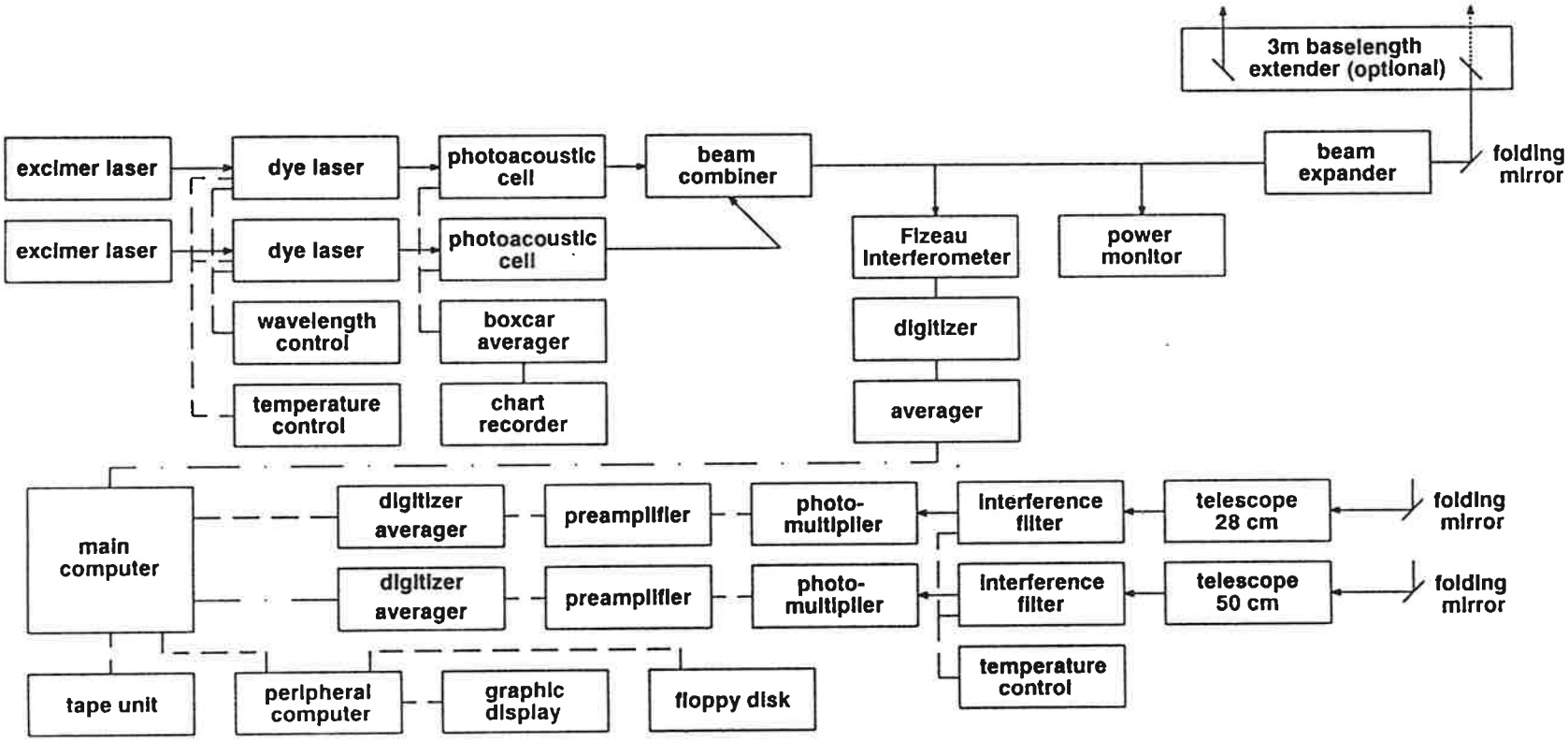

Fig. 2 DIAL System overview

and 2 amplifier stages. Wavelength stability is achieved by mounting the the tuning elements of the oscillator, a 600 grooves/mm grating used in 4^{th} order and a $0.75cm^{-1}$ FSR air spaced etalon, in a closed compartment which is temperature controlled by a constant temperature liquid flow system. Wavelength tuning is done by a coordinated tilt of both etalon and grating under computer control. The resolution depends on the tilt of the etalon due to its nonlinear tuning curve, in the used range it is better than 0.1 pm. About 0.7 nm can be scanned by etalon tilt without readjustment.

The basic parameters of the optical system are listed in table 1. It should be noted, that at the present level of complexity of the whole system usually not all subsystems are operated under optimum conditions simultaneously. So typical performance data are shown rather than manufacturer specifications.

The two dye lasers are operated at different polarization, in one laser the plane of polarization as determined by the optical elements of the oscillator is rotated by means of a half wave plate between the first and the final amplifier stage. Each beam is passed through a photoacoustic cell filled with approximately 16 hPa of water vapor (saturation pressure at room temperature) providing a convenient means for wavelength tuning to the maximum of the absorption line chosen for the particular experiment and allowing a continuous check of the wavelength setting [30]. The output of the photoacoustic cells is analyzed with a boxcar averager and presently recorded on strip chart. At this low pressure the lines are narrow ($\approx$ 3 pm FWHM), so the output of the photoacoustic cell is rather sensitive to small laser line drift.

Combination of the 2 beams is performed by a Glan type polarizer operated in reverse. It is important, that after combination the 2 beams point into the same direction very precisely, so the polarizer was mounted on an ultra high precision 2 axis tilt stage. The fine adjustment is controlled by observing the ratio of averaged return signals as a function of height, with both lasers tuned to the same off line wavelength. This ratio is constant with height only if the overlap functions of both beams are the same, deviations from this are easily detected.

Fig. 3 shows an example for an upper tropospheric measurement. Both signals and the log of the ratio of the two signals are displayed, the latter on a very expanded scale. From this figure we can see, that the log of the ratio stays constant mostly within ± 0.01, with the exception of a system-

Table 1: System parameters

Transmitters, 2 Excimer pumped dye lasers	
output energy	35 mJ
bandwidth FWHM	1.5 pm
spectral impurity	$< 2\%$
repetition rate	12 Hz typical, 24 Hz tested
beam dimensions	$2 \cdot 2$ mm
beam divergence (prior to expansion)	1.5 mrad
beam expansion	$\times 15$ (optionally $\times 25$ or $\times 35$)
Bandwidth measurement, Fizeau interferometer	
resolution of readout	0.1 pm
optical resolution, FWHM	0.8 pm
Receiving optics	
Schmidt Cassegrain telescope, diameter	0.28 m
Newtonian telescope, diameter	0.5 m
distance transmitter-receiver	0.3 m
	3.0 m optionally
filter bandwidth	8 nm
	0.6 nm optionally

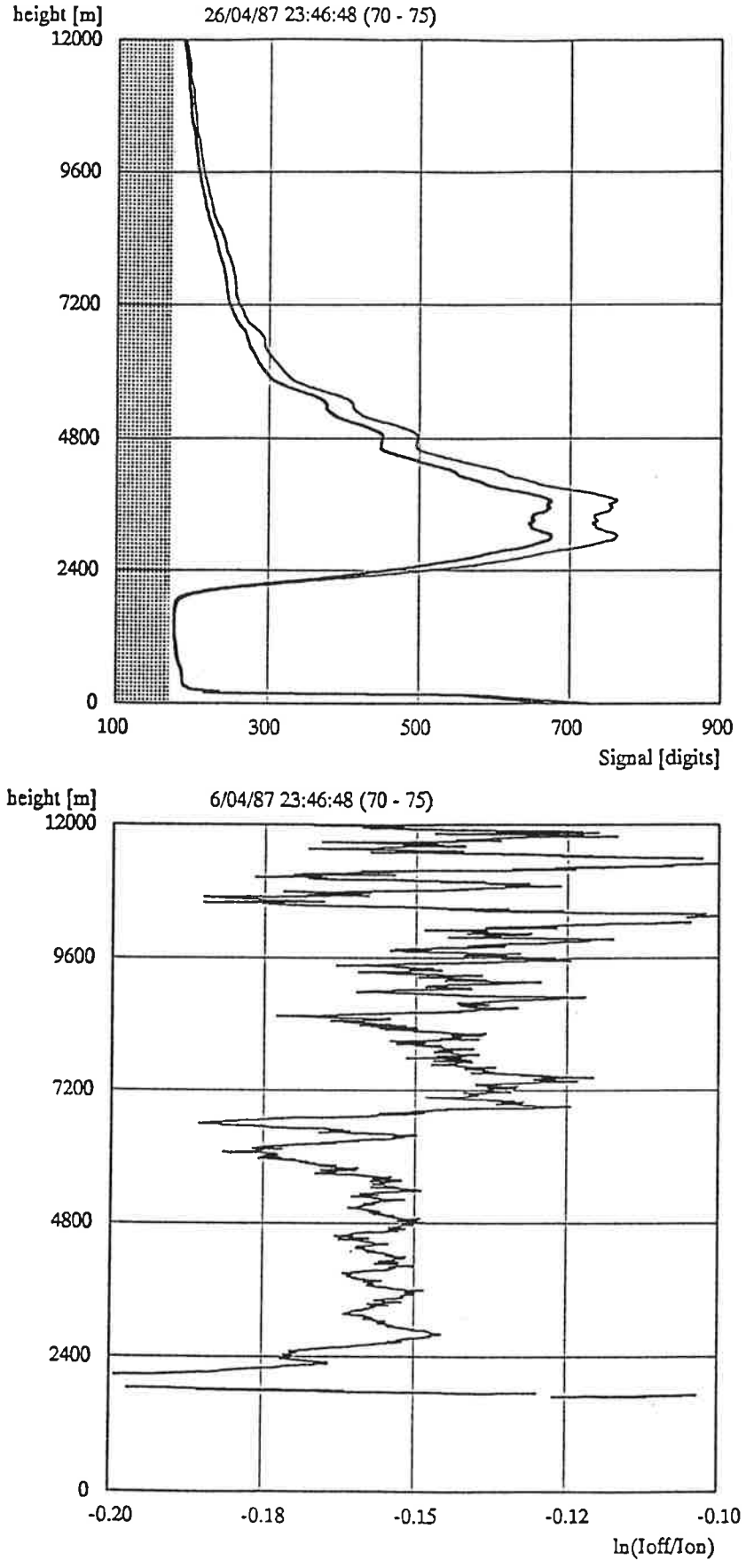

Fig. 3a (top) and Fig. 3b (bottom) On and off line signals (a) and optical depth $\tau = \ln(P_{off}/P_{on})$ (b) for a test case with $\lambda_1 = \lambda_2 = \lambda_{off}$

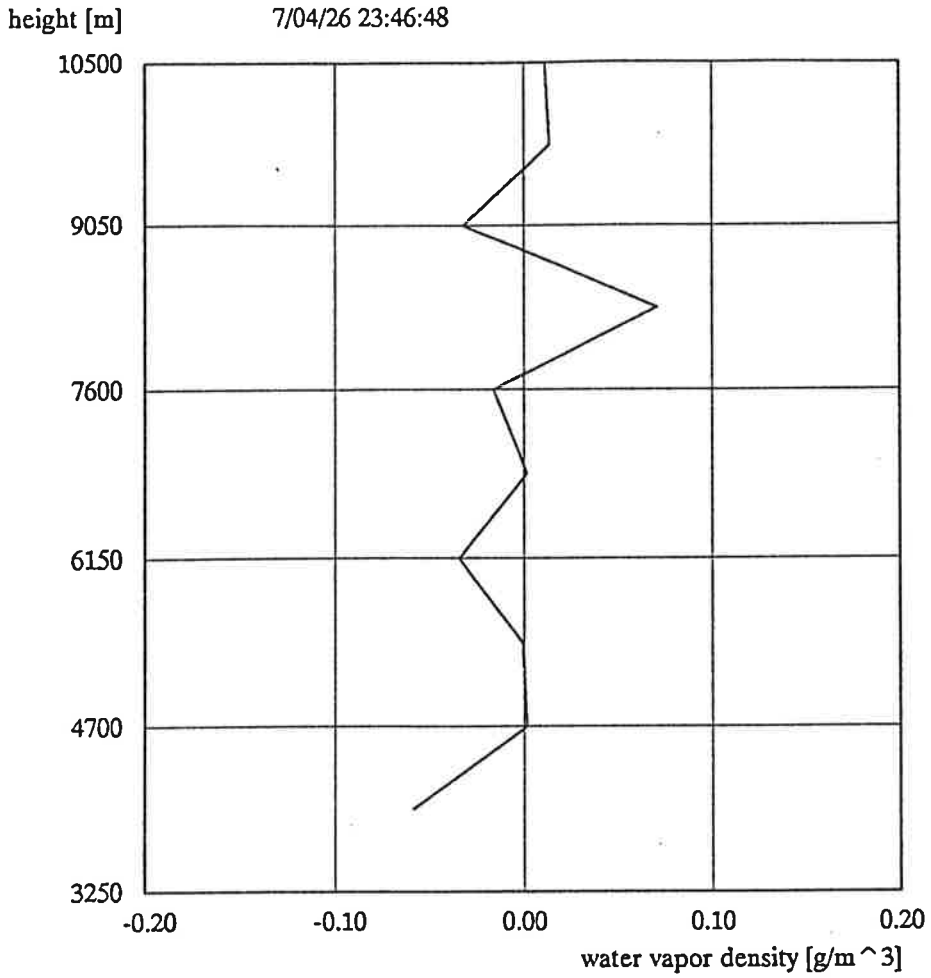

Fig. 3c Equivalent water vapor density for the case of fig. 3b.

atic pattern at $\approx 7000m$, where the deviations reach 0.02. This pattern is basically constant with time and appears to be associated with the central obstruction of the telescope. Consequently, the actual measurements can be corrected for this deviation if necessary. Figure 3c shows the error in water vapor retrieval associated with these deviations from a constant value, using the same line parameters as for the real online - offline measurement. The error basically stays below $0.02g/m^3$, with larger systematic errors only at the lowest end of the range, and at $\approx 8000m$, as already discussed. This result is very satisfactory.

The different linear polarization of both transmitted beams is subsequently transformed into circular polarization by means of a quarter wave plate to avoid errors due to differences in the backscatter coefficient for different polarizations, which might occur for special backscatter situations (e.g. oriented ice crystals).

A small fraction of the beam is picked off for power monitoring and spectral analysis, which is done by a multibeam Fizeau interferometer with photodiode readout for every shot. The resolution of the readout is 0.1 pm, the FWHM of the instrument response as tested with a single longitudinal mode HeNe laser is 0.7 pm. The output of the photodiode array is digitized and averaged over a large number of shots to provide an information on the effective linewidth of the laser, including short term drift. Finally, the combined laser beams are expanded, usually $\times 15$ ($\times 25$ or $\times 35$ optionally), and transmitted vertically into the atmosphere using a 45° folding mirror with hard dielectric coating. This folding mirror can be moved to a position $\approx 3m$ further out, to increase the distance between the transmitted beam and the telescope axis. This is done to suppress the close range return signals, because the strong overload associated with these signals cause memory effects in the photomultiplier at the high gain necessary for the detection of far range signals. The easiest way to avoid this is to start overlap between transmitter and receiver field of view at sufficient height only, well above the boundary layer with its usually rather large aerosol content. The overlap function is controlled by the baselength and the tilt of the transmitted beam with respect to the telescope axis. This is done at the beginning of each experiment, the height where the overlap starts is easily determined visually from the shape of the return signal averaged over a sufficient number of shots. The receiving optics starts with 2 large 45° folding mirrors mounted to the same rigid frame as the folding mirror for the transmitted beam. Each mirror directs the scattered

light to a telescope with $0.28m$ and $0.50m$ diameter, respectively. These 2 telescopes allow observations at 2 different overlap function settings and different gainsettings simultaneously, a feature which has not yet been used since the second data acquisition channel is going to be implemented only now. In both telescopes the field of view is determined by a diaphragm in the focal plane, after expansion to $30mm$ diameter the beam is passed through an interference filter. For boundary layer or night time measurements usually a $7nm$ bandwidth (FWHM) is sufficient, for upper tropospheric measurements a $0.6nm$ filter is used, mounted in a temperature controlled oven on a tilt stage allowing exact tuning to the wavelengths used.

3.3 Detector, electronics, and data acquisition

As a detector in both channels a photomultiplier tube (RCA 8852) is used followed by a fast preamplifier (Analog Modules 310-3, 3 db cutoff frequency 14 MHz). A 20 MHz 12 bit transient recorder (DSP 2112F) digitizes the signals. Of the 8k samples recorded by the transient digitizer for each shot pair, only the interesting parts of the signal are transferred to the computer (National Semiconductor 32016 boards on a Multibus structure). This includes pretrigger samples for background detection (typically 50 samples for boundary layer measurements, 250 samples for upper tropospheric measurements). The rest is split between the return of the first and the second laser, which are fired with $200\mu sec$ separation. After transfer to the computer the data are checked for overloads, and for each range bin only valid signals are accumulated. All parameters are software selectable and chosen in the setup menue.

For detailed data analysis following the experiment usually 100 shot averages of the return signals from both lasers are stored on magnetic tape together with time and housekeeping information. The online system is capable of displaying line graphs of the 2 return signals and the logarithm of their ratio. Zoom functions are available on all axes, and the number of shots averaged can be selected as multiples of the hardware averages (which themselves can be chosen arbitrarily). These capabilities are necessary for the setup procedures, where the timing and the overlap between the transmitted beams and the field of view of the telescope have to be adjusted. During the measurements this display provides very valuable information about the meteorological situation as well as the system condition. The displayed data

are stored on floppy disk as a backup and easily accessible data source for later evaluations on a low cost PC.

Time synchronisation of the two lasers requires some attention.When steep gradients are present in the backscatter profile, timing errors between the 2 shots of only a fraction of the sampling interval produce large errors in the ratio of both signals and hence in the concentration to be evaluated. Both laser triggers are controlled by the same high precision pulse generator, the delay between the 2 triggers can be set with a precision of better than $1nsec$. In the excimer lasers switching circuit a delay occurs between trigger and actual laser firing, which is strongly dependent on the operating conditions of the thyratrons and may vary over several tens of nsec within half an hour. Moreover, this trigger delay drift is different for both lasers. To avoid this drift, a feedback loop was installed in each laser (Lambda Physik EMG 97) which stabilizes the trigger to firing delay. The actual delay between the 2 laser pulses is measured continuously using a fast photodiode and a counter/timer. It is set to an exact multiple of the sample interval of the digitizer to have the same phase for both shots with respect to the digitizer sampling. The stability of the whole circuit is better than $2nsec$ over several hours.

3.4 Capabilities for depolarization measurements

As an option, the whole system can be operated in a different mode to measure the depolarization of the backscattered signal, which is interesting for studies of cloud microphysical properties. When the 2 lasers are operated at the same off line wavelength, the quarter wave plate after the beam combiner is ommitted, and a polarizer is inserted in the receiver optics, the system is ready for a depolarization measurement. While in the usual depolarization setup only one pulse is transmitted, and the analysis is done in 2 channels with orthogonal planes of polarization, in our system the 2 transmitters are operated at different planes of polarization, detection is done with one channel only. So for one pulse the plane of the detector polarizer is parallel to that of the transmitted light, for the other pulse it is perpendicular. If the scattering by the particles under consideration does not depend on the polarization of the incident light, which may be assumed either for particles with spherical symmetry or for an ensemble of randomly oriented particles with arbitrary symmetry properties, both setups are equivalent. It may be emphasized that

both signals are obtained quasisimultaneously as already discussed for the DIAL measurements. This is very important for measurements in clouds, too, because the backscatter coefficient often is highly variabel in time and space.

The rest of the system remains unchanged, especially the data acquisition system, which is more than adequate for this type of measurements. First results have been presented in a separate paper [31, 32].

4 Tests of adjustment

For many parts of the system easy procedures exist to find and maintain the correct settings for their adjustment. For the alignment of the two laser beams with respect to equal overlap with the telescope field of view, and for the adjustment of the online laser with respect to minimum spectral impurity, special test procedures had to be developed. For the overlap, the method has been described in section 3.2.

Spectral impurity is determined using DIAL measurements with one laser tuned to off line as usual and the other one tuned subsequently to 2 different lines with different line strengths. Fortunately this has been possible for the lines chosen for the actual measurements within the scanning range of the intracavity etalon, so the complete adjustment could be maintained. The ratio of both optical depths should be constant with height, deviations occuring at greater depth indicate the level of spectral impurity. The accuracy of this determination is limited because of the variability of the water vapor column content, since both measurements cannot be made simultaneously. Fig. 4 shows an example for a boundary layer measurement. The observed ratio of optical depths is well reproduced by calculations using eq. 4, $\tau_2 = \tau_1 \cdot (\sigma_2/\sigma_1)$, and $P_b = 0.018$, where σ_i are the appropriate absorption cross sections. The large deviations from the calculated curve above $1.4km$ are due to errors caused by the low signal for the stronger line (τ_2), while the smaller deviations below are easily explained by the time difference of $5min$ between the 2 measurements of τ_1 and τ_2 involved. 1.8% spectral impurity, as determined for this case, limit the usable range of optical depth for DIAL measurements with an error less than 10% to $\tau < 1.8$. Assuming that the determination of the spectral impurity is accurate to 0.5% for the whole time of the measurement, by correction the usable range could be extended to $\tau < 2.3$ for the

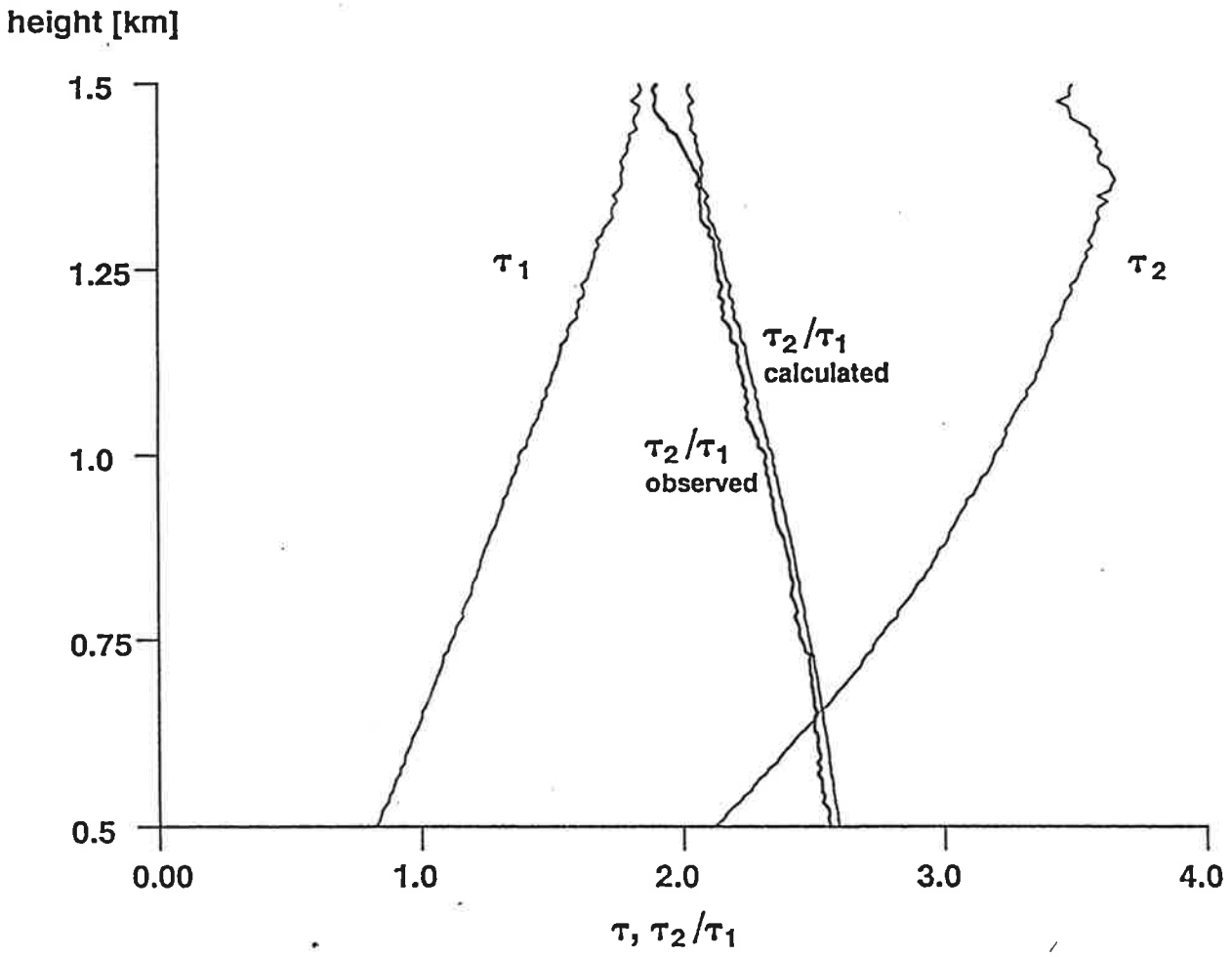

Fig. 4 Observed optical depths τ_1 and τ_2 for the line pair 724.3717nm and 724.3477nm. τ_2/τ_1 calculated from τ_1 for 1.8% spectral impurity. 09/16/1987 13:41 GMT

same error. It should however be kept in mind, that spectral impurity is not necessarily constant for the whole time of a measurement series.

5 Examples of measurements

It is obvious, that the DIAL system is fairly complex in hardware as well as in the evaluation scheme. Its performance depends critically on a number of parameters. Some of these parameters can be measured independently with sufficient accuracy, the well understood DIAL methodology then helps to determine the errors produced by the uncertainty in these parameters and to avoid them by proper system design. Other important parameters depend critically on the adjustment of the optical system, namely spectral impurity and the geometrical overlap function of the 2 transmitted beamswith the telescope field of view. Test methods for these quantities have been described above.

Because of the complexity of the systems, its overall accuracy remains to be assessed. This turned out to be rather difficult, mainly because of

- the lack of easily accessible accurate instruments (e.g. the accuracy of radiosoundings is not well established, at least at greater heights, say $> 5km$, and after passage through clouds)
- the different sampling properties; none of the conventional measurement systems has nearly the same probe volume as the Lidar.

In spite of these difficulties, the following examples will demonstrate the present performance of the Lidar system.

5.1 Low altitude measurements

The best situation for intercomparison with in situ instruments is for a horizontal path. We have been able to perform such a measurement during the International Cirrus Experiment 1989 on the island of Sylt, with the beam pointing over flooded tidal flat areas at $\approx 35m$ height. Fig. 5 shows the results of several Lidar measurements using different absorption lines, in comparison to the ground level psychrometer reading. The situation was constant for a quite long time, it is rather unlikely that strong horizontal or temporal differences occurred. The results show

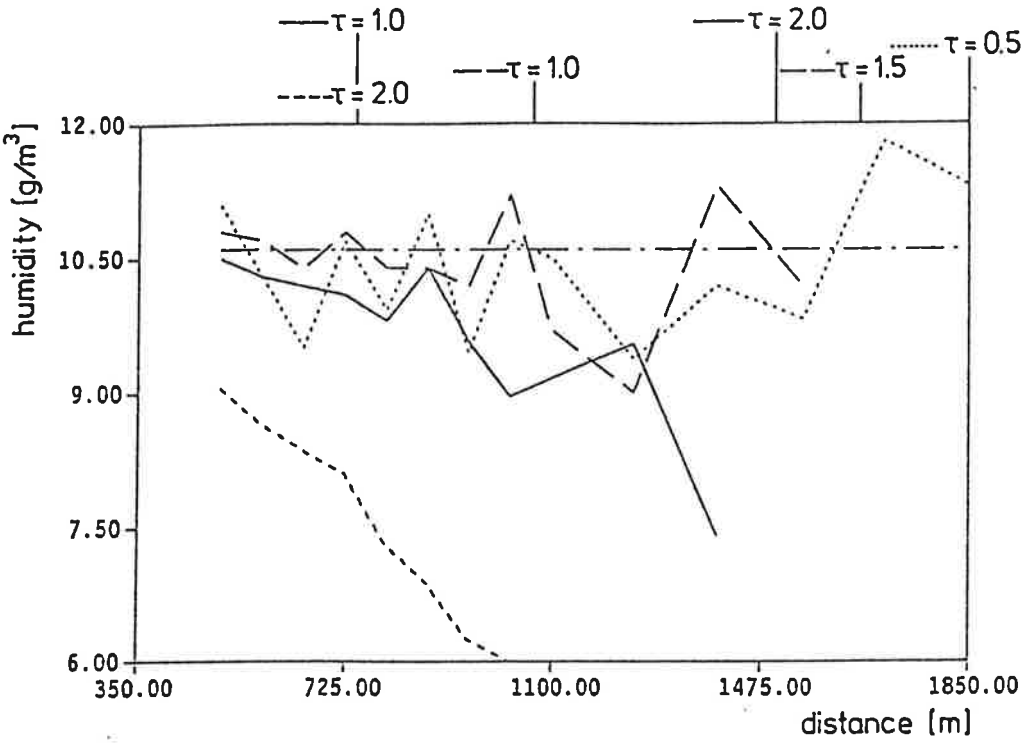

Fig. 5 Horizontal DIAL measurement with 4 different absorption lines, compared to psychrometer (—·—).

——— : $\lambda = 728.8126nm, S = 7.24e-24cm/mol$

– – – – – – : $\lambda = 728.7379nm, S = 14.95e-24cm/mol$

····· : $\lambda = 728.3214nm, S = 1.36e-24cm/mol$

— — — : $\lambda = 728.2282nm, S = 4.50e-24cm/mol$

- reliable results can be obtained up to an optical depth $\tau \approx 2$, due to the spectral impurity of the laser
- in this region the accordance between different Lidar measurements and the psychrometer reading on the average is better than 3%
- if a weak absorption line is used, the statistical error increases, in the present case up to 10%, because the differential optical depths are small and can only be determined with limited accuracy
- only sufficiently large signals (greater than ≈ 10 digitizer bins) can be evaluated. For smaller signals systematic errors of the digitizer cause unacceptably large errors in the results.

If a proper absorption line is selected, for a certain range good absolute accuracy can be achieved if and only if the actual spectral distribution of the laser is taken into account. The possible range is determined by the spectral purity of the laser and the dynamic range of the signal.

The next example, fig. 6, shows the intercomparison of a Lidar vertical sounding with the dewpoint mirror (which is generally regarded as the most reliable humidity sensor) on board of the DLR research aircraft "Falcon", and a radiosonde which was launched locally directly after the aircraft passage. The difference betweentheLidar and aircraft at the flight level of $1430m$ is less than 5%. The differences between Lidar and radiosonde are larger at some height ranges. At least to some extent this can be explained by the different sampling properties of the instruments, the sonde trajectory is definitely different from the Lidar path, and both temporal and vertical resolution are different. Overall, the instruments compare well, and particularly the Lidar-aircraft intercomparison, which is regarded as most meaningful with respect to sampling properties and reliability of the instrument, is very favorable for the Lidar. Unfortunately, not more well designed intercomparison flights could be organized up to now.

The last example for lower tropospheric measurements will demonstrate how this system can be used for high resolution studies of atmospheric processes in the boundary layer. The measurements were taken on the island of Sylt close to the shoreline of the North sea, the meteorological situation was characterized by the passage of a weak cold front just before the measurements started. A westerly wind was blowing directly from the open sea with

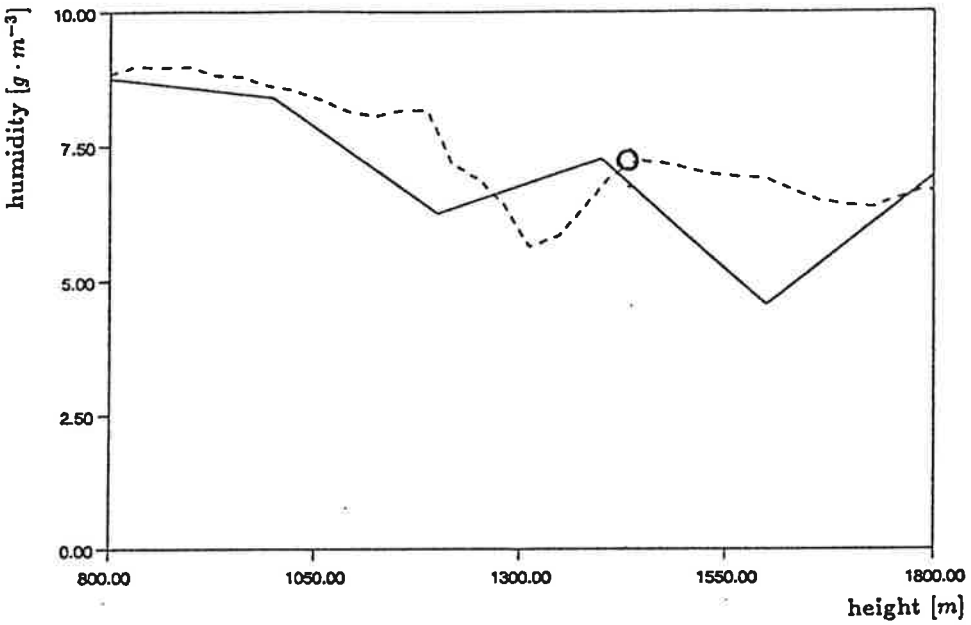

Fig. 6 Intercomparison of DIAL humidity measurements (solid line) with aircraft (circle: dewpoint mirror on DLR-Falcon) and radiosonde (broken line). Aircraft height $1430m$, speed $107m/sec$.

$\approx 10m/sec$. In the beginning the boundary layer was only shallow ($\approx 500m$), subsequently small cumuli provided for sufficient mixing to raise the boundary layer to $\approx 1600m$). These informations have been retrieved both from locally launched radiosondes and the analysis of the Lidar backscatter signal.

Fig. 7 shows the time series of both range corrected signal and retrieved water vapor density, simultaneously in three height levels, with a resolution of 25 sec in time and 75 m in height. Increased humidity is observed in the regions below the cumuli, which are easily detected from the backscatter signal. In addition a number of downdrafts is observed, where rather dry and clean air is transported downward. This occurs in relatively small regions mostly at the cloud rims, and continues for several hundred meters below cloud base. For these events the humidity is highly correlated at all measurement heights. In addition, humidity is also highly correlated with the backscatter signal. This certainly has two reasons: the air mixed from the upper layers is cleaner and thus has a smaller backscatter coefficient, and it is drier, so the particles are less grown by water adsorption.

It should be mentioned, without going into all details, that the observed general decrease of absolute humidity with time, and the rise of cloud base, are consistent with ground level observations. So from all these observations it can be concluded, that the system is well suited for studies of atmospheric processes like the convective situation shown here.

The measurement shown above has also been used to estimate the relative accuracy of the high resolution water vapor retrieval. Fig. 8 shows a variance spectrum of the humidity time series at 247 m height from the above measurement. The form of the spectrum looks quite reasonable, it shall not be used here to derive any meteorological properties. For the given method of DIAL- measurements, the noise spectrum should be white. Then the spectral density of this noise must be smaller than the lowest significant level of the observed spectrum. This is a safe upper limit for the system noise, assuming that in the lowest part of the spectrum the meteorological contribution is neglible. For the given case, the lowest significant level, which is observed at the high frequency end (as expected), corresponds to a white noise with a standard deviation of $0.11gm^-3$. For the case shown, this corresponds to a relative error of 1.6%, which is very satisfactory. This again demonstrates quite clearly that the system is suitable for studies of even rather small scale convective processes in the boundary layer.

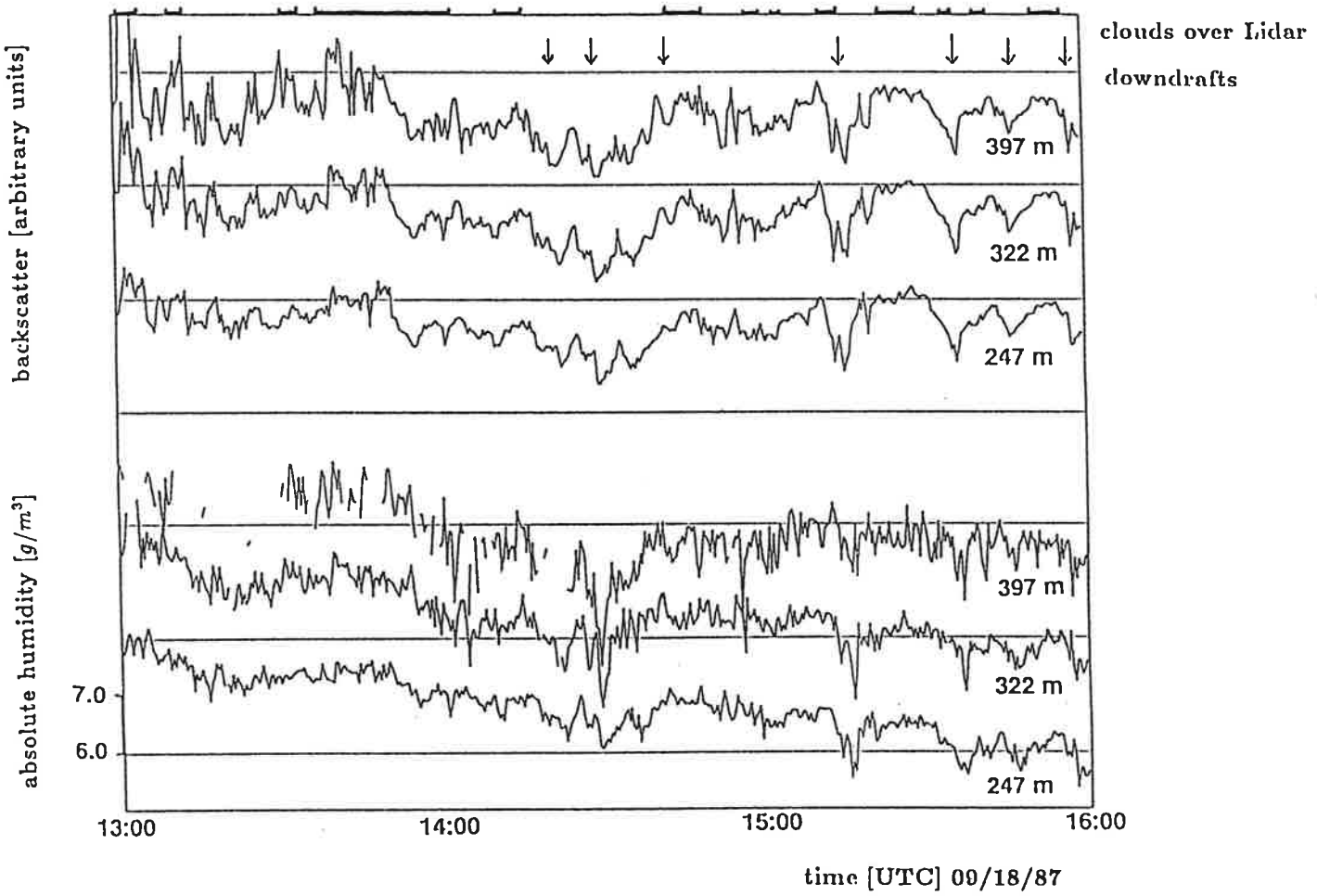

Fig. 7 Time series of backscatter signals (top) and humidity (bottom) for three different levels. Regions with clouds are marked at the upper edge of the figure, as well as "downdrafts".

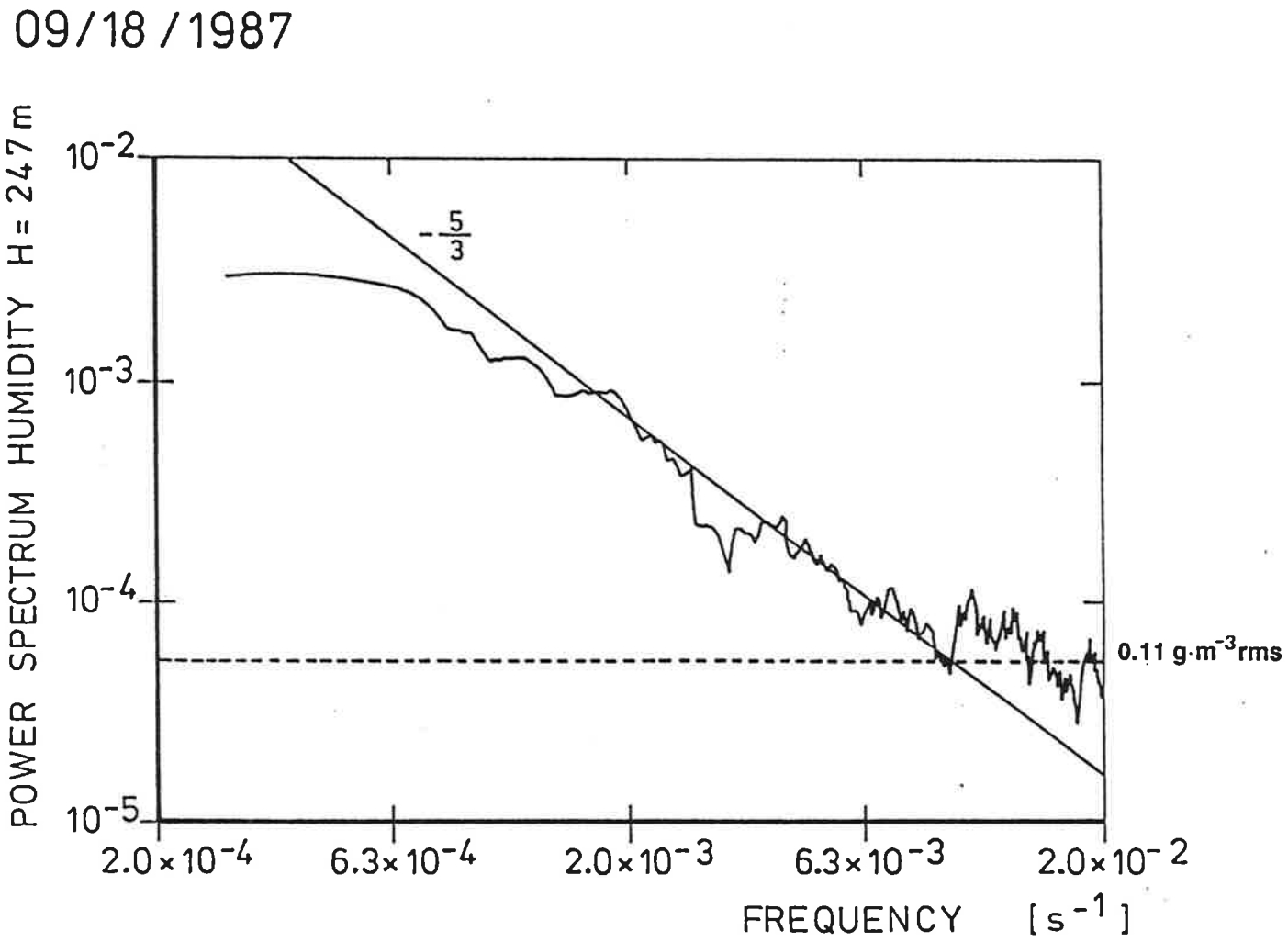

Fig. 8 Variance spectrum of humidity for the case of figure 7 at 247m height. The broken line indicates assumed maximum level of noise.

5.2 Upper tropospheric measurements

Measurements in the upper tropopshere are much more difficult than at lower altitude. The main reasons for this are

- absorption lines are much narrower at low pressure
- signals are several orders of magnitude lower
- spectral impurity sets limits to the allowed optical depth up to the observing height
- water vapor density is much higher in the lower troposphere, so small changes in optical depth have to be detected in the upper troposphere after strong attenuation in the lower troposphere

These difficulties could not yet be solved to come up with routine water vapor measurements in the upper troposphere, so far measurements are restricted to favorable cases. Two examples will be shown to demonstrate the present performance of the DIAL system.

The first example is a night time measurement in a calm, cloudless night. Weather maps showed that the air mass was rather homogeneous over an extended area. Fig. 9 shows a Lidar measurement compared to a radiosounding of the German weather service launched at Schleswig, about $90km$ north of the Lidar site. The resolution of the Lidar measurements is 500 - $1000m$, the height range 4 - 8 km. The measurements were continued for 3.5 hours, no significant changes were observed during this time. The difference between Lidar and radiosounding is $< 20\%$. Even for the rather horizontally homogeneous situation a better accordance cannot be expected.

For an inhomogeneous distribution of the backscatter coefficient the measurements are more difficult. First, the dynamic range of the signal is increased, leading to problems in the accuracy of acquisition of strong and/or weak signals. Second, long averaging times cannot be accepted, since the situation may change considerably within the measurement time. Third, Rayleigh-Doppler corrections are quite different at different heights, requiring accurate determination of input parameters for the correction scheme. These difficulties are illustrated in the last example, which was picked out of a 3 hours measurement period obtained during the International Cirrus Experiment 1987, when a warm front was approaching the lidar site. The

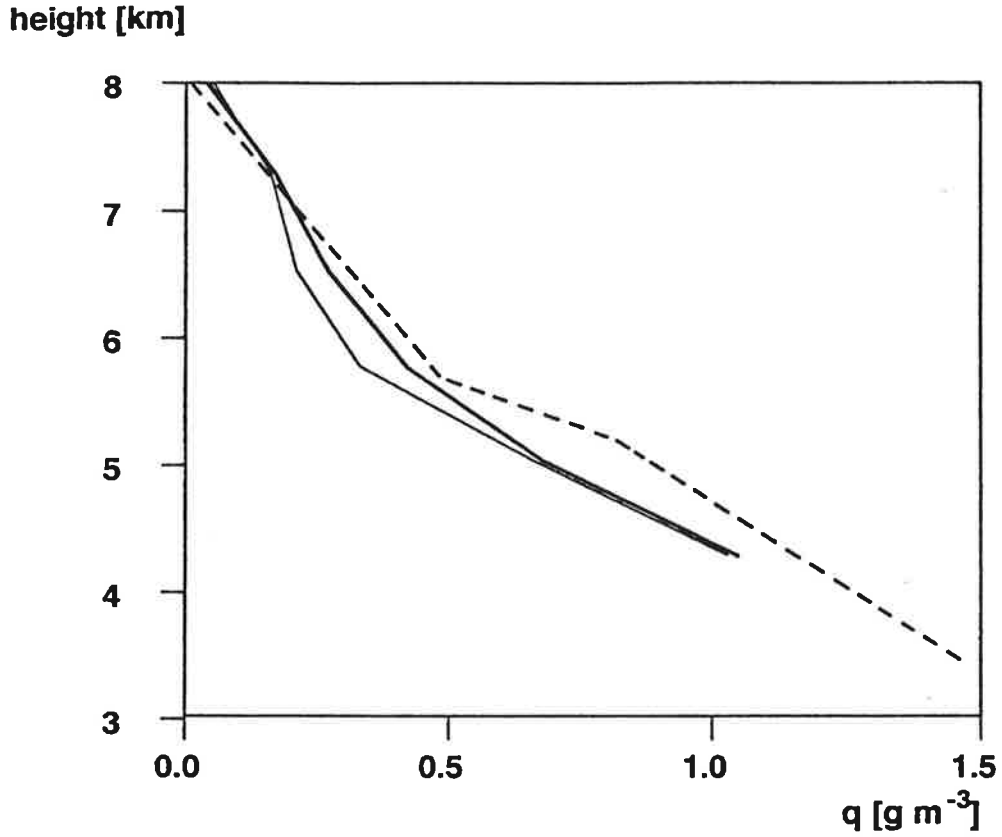

Fig. 9 Water vapor profiles measured on 04/26/1987, 22:27 GMT. Thick solid line: DIAL with Doppler correction for molecular scattering. Time average $27min$, range resolution $750m$. Broken line: DIAL without Doppler correction. Thin solid line: Radiosonde ascent 04/27/1987 00:00 GMT, $90km$ north of the lidar site

backscatter coefficient retrieved from the off-line signal using the algorithm described by Fernald [33] is shown in fig. 10. The dominant feature is the cirrostratus layer extending from $5km$ to $\approx 10km$, where the backscatter coefficient is about 2 orders of magnitude larger than the molecular scattering. Below this, there is a layer of very clean air for $4km < z < 5km$, and 2 more layer boundaries may be derived from the associated peaks in the aerosol backscatter at $\approx 3.8km$ and $\approx 2.9km$. In the profile of $\ln(P_{off}/P_{on})$, shown in fig. 11, these layers can be found as well, exhibiting different slopes in the individual layers. It is seen, too, that the low signal from the clean layer $4km < z < 5km$ makes the accurate determination of water vapor difficult for this region, the logarithm of the signal ratio shows considerable noise and small slope. Analysis of the signal strength in this region indicates, that lack of accuracy in the data acquisition system may have considerable influence. Using the information from the backscatter profile concerning the layer structure, an average water vapor concentration may be determined for the complete layer, calculating the total optical depth of the layer as a difference from the boundary values of the adjacent layers. As the scattering mechanisms contributing to the signals are quite different in the different regions, Doppler correction is fairly important. The main problem then is to determine the correct amount of aerosol scattering for $z < 5km$. When integrating from the top through the cirrus layer, small errors in the assumed value of the backscatter to extinction ratio in the cirrus layer lead to unreasonable values in the region below. So the backscatter retrieval had to be performed in 2 separate steps for the cirrus and the subcirrus regions. The start value of the aerosol backscatter for the lower layer, which has to be guessed, has considerable influence on the results for this region. As long as no further information is available, this limits the accuracy of the aerosol backscatter coefficient in the subcirrus region, and therefore the accuracy of the Doppler correction for the water vapor retrieval.

In fig. 12 the retrieved water vapor profile is shown, with estimates of random and systematic errors. Rayleigh Doppler correction is very important only in the region between $4km$ and $5.5km$. Over most of the range, signal noise remains the dominant error source. Quite generally, the individual contributions to the error budget stay well below 10%. The comparison with a radiosonde ascent made at the same site at 16:00 GMT shows good agreement in the basic structure of the troposphere, with the most striking deviations in the range frome 3.5 - $6.5km$. For this particular range, the

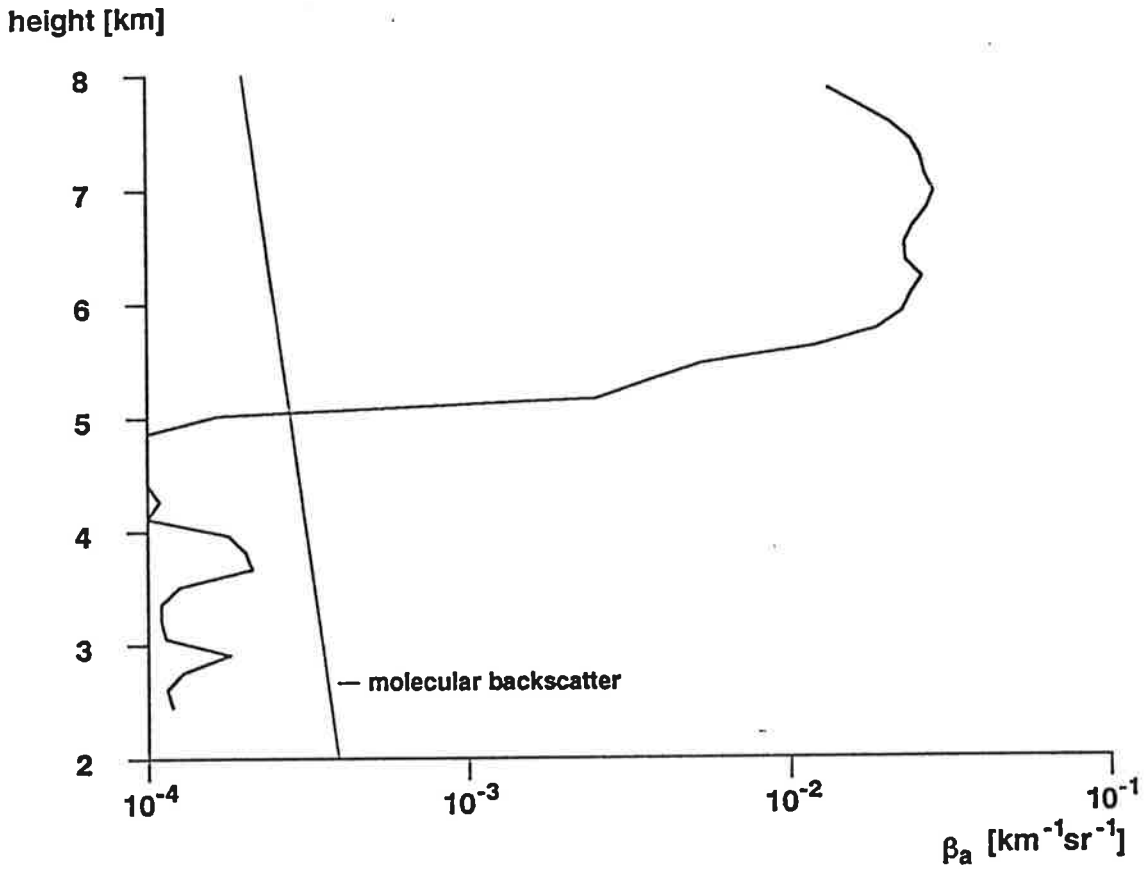

Fig. 10 Nonmolecular backscatter, retrieved from the off line signal. 09/19/1987 20:08 GMT. Time average $5.5min$, height resolution $150m$. Molecular backscatter calculated from density profile according to radiosonde ascent 16:00 GMT

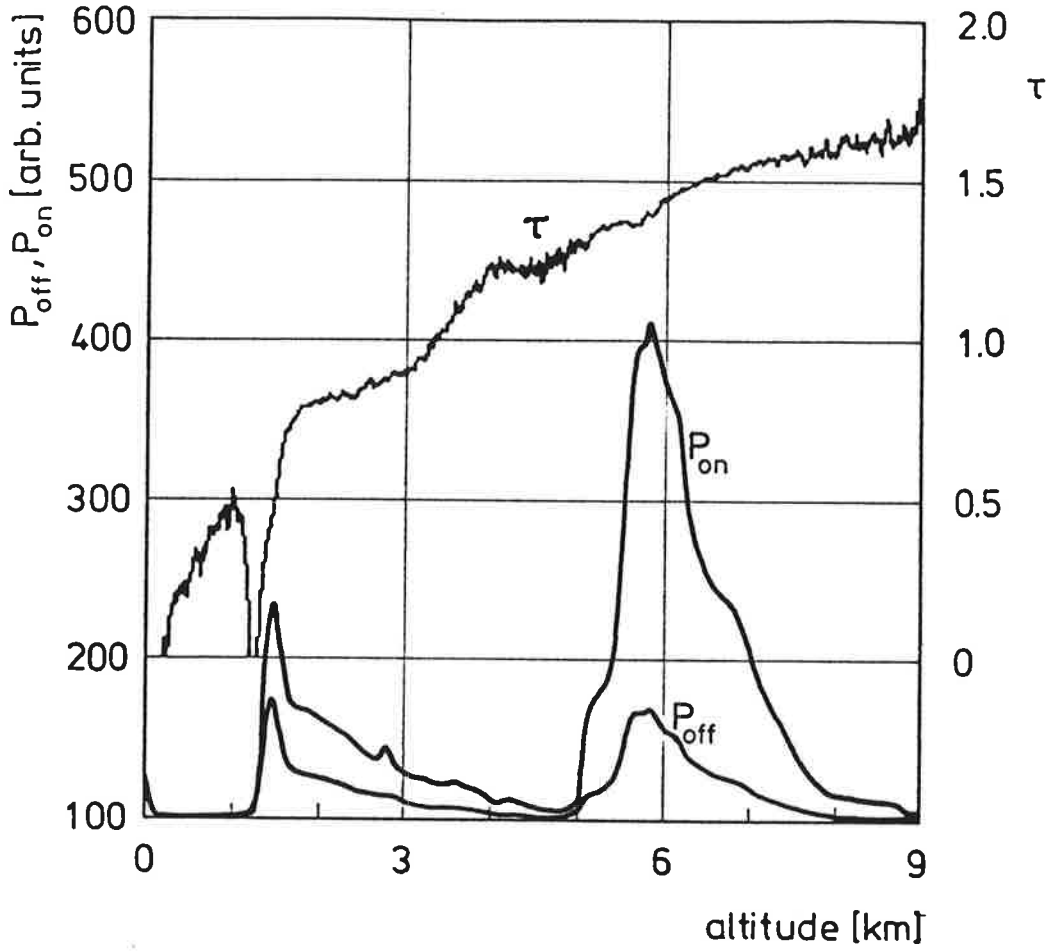

Fig. 11 On and off line signals, and $\tau = ln(P_{off}/P_{on})$ for a DIAL measurement 09/19/1987 20:08 GMT. Time average $5.5min$, smoothed with a $67.5m$ gliding average.

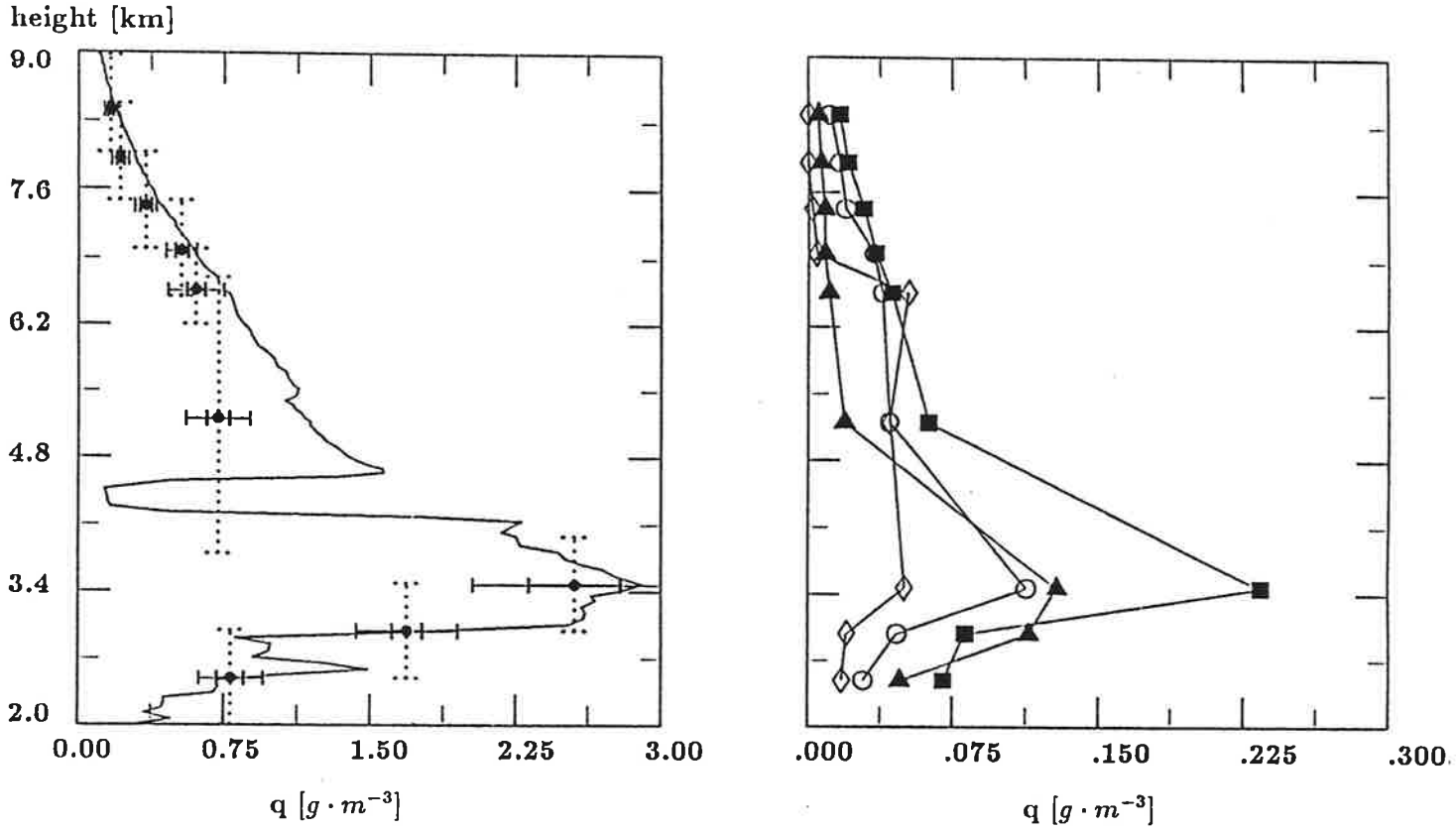

Fig. 12 **Humidity measurement in cirrus, 09/19/1987 19:07 GMT.**

Left: absolute humidity measured by Lidar (·) and radiosonde (—). Small error interval: signal noise only. Large error interval: largest possible error including all known systematic errrors. Vertical bar: height intervals used for each measurement. Right: systematic errors due to △ correction for beam geometry, ◇ Rayleigh Doppler effect, ○ spectral impurity, □ signal noise.

Lidar backscatter signal strongly supports the layer structure retrieved from the DIAL measurements, so the difference is ascribed to problems with the radiosonde, either with its reliability or with the different path through the atmosphere. Accounting for the variability of the atmosphere, the agreement between lidar and radiosounding is remarkably good.

In spite of the difficulties associated with a measurement in an inhomogeneous atmosphere, the results give a lot of information about the meteorological processes involved. In particular, a detailed analysis of the whole measurement interval from which the example was picked, allows the determination of :

- the extent of the cirrus layer
- the structure of the subcirrus region
- the absolute and relative humidities in separate regions of the cirrus layer, especially in the lower, unsaturated part (It should however be mentioned, that the accuracy and particularly the height resolution is not sufficient to study the details of the icing process).

For the present case, all these informations have been obtained with a time resolution of $5.5min$ for a period of 3 hours (with some interruptions for system tests and slight readjustments), clearly demonstrating that the lidar is a unique instrument for studies of these processes, since the same information cannot be obtained by any other system.

6 Summary and conclusion

A water vapor DIAL system has been described which has been demonstrated to be a versatile instrument for the investigation of meteorological processes in the troposphere. High temporal resolution has been achieved (30 sec in the boundary layer, 5 - 30 min up to 10 km height), combined with a vertical resolution of $75m$ in the lower and $1km$ in the upper troposphere. The possible sources of error have been studied to some detail, and their influence on the resulting accuracy of the measurement have been discussed. Test methods for the correct adjustment of the whole system have been described, too. Although the adjustment of the complete system to the required accuracy is a fairly big effort, the results are very encouraging and cannot

be obtained by any other method. Particularly for the upper tropospheric measurements, technological improvements expected for the next future will considerably enhance the applicability of the system. We will continue to study meteorological processes in the troposphere with this system.

Acknowledgement: The author would like to thank H.Hinzpeter for initiating and continuously supporting this project.

It is obvious, that a complex system like the one described in this paper could only be built as a joint effort of a larger team. The valuable contributions of A. Ansmann, H.Linné, M. Pfeiffer, V. Rohde, J. Sakreida, F. Theopold, as well as the whole engineering and technical staff of the institute are gratefully acknowledged.

The project was supported financially by the Bundesminister für Forschung und Technologie under grants KF 10056 and KF 10110.

References

[1] E. V. Browell, T. D. Wilkerson, T. J. McIlrath: "Water vapor differential absorption lidar development and evaluation" Appl. Opt. 18, 3474-3483 (1979)

[2] Ch. Werner and H. Herrmann: "Lidar measurements of the vertical absolute humidity distribution in the boundary layer" J. Appl. Met. 20, 476-481 (1981)

[3] C. Cahen, G. Megie, P. Flamant: "Lidar monitoring of the water vapor cycle in the troposphere" J. Appl. Met. 21, 1506-1515 (1982)

[4] V. V. Zuev, V. E. Zuev, Yu. S. Makushkin, V. N. Marichev, A. A. Mitsel: "Laser sounding of atmospheric humidity: experiment" Appl. Opt. 22, 3742-3746 (1983)

[5] E. V. Browell, A. K. Goroch, T. D. Wilkerson, S. Ismail, R. Markson: "Airborne DIAL water vapor and measurements over the gulf stream" 12th International Laser Radar Conference, 151-156 (1984)

[6] E.R. Murray: "Remote measurement of gases using differential absorption lidar" Opt. Eng. 17, 30 (1978)

[7] K.W. Rothe: "Monitoring of various atmospheric constituents using a cw chemical hydrogen/deuterium laser and a pulsed carbon dioxide laser" Radio Electron. Eng. 50, 567 (1980)

[8] P. W. Baker: "Atmospheric water vapordifferential absorption measurements on vertical paths with a CO_2 lidar" Appl. Opt. 22, 2257-2264 (1983)

[9] R. M. Hardesty: "Coherent DIAL measurement of range-resolved water vapor concentration" Appl. Opt. 23, 2545- 2553 (1984)

[10] W.B. Grant, J.S. Margolis, A.M. Brothers, and D.M. Tratt: "CO_2 DIAL measurements of water vapor" Appl. Opt. 26, 3033 - 3042 (1987)

[11] S.H. Melfi, J.D. Lawrence, Jr., and M.P. McCormick: "Observation of Raman scattering by water vapor in the atmosphere" Appl. Phys. Lett. 15, 295 - 297, (1969)

[12] J.A. Cooney: "Remote measurements of water vapor profiles using the Raman component of laser backscatter" J. Appl. Meteorol. 9, 182 - 184 (1970)

[13] R.G. Strauch, V.E. Derr, and R.E. Cupp: "Atmospheric water vapor measurement by Raman lidar" Rem. Sens. Environ. 2, 101 - 108 (1972)

[14] J. C. Pourny, D. Renaut, A. Orszag: "Raman-lidar humidity sounding of the atmospheric boundary-layer" Appl. Opt. 18, 1141-1148 (1979)

[15] S.H. Melfi and D. Whiteman: "Observation of lower-atmospheric moisture structure and its evolution using a Ramanlidar" Bull. Am. Meteor. Soc 66, 1288-1292 (1985)

[16] D. Renaut, J. C. Pourny, R. Capitini: "Daytime Raman-lidar measurements of water vapor" Optics Letters 5, 233- 235 (1980)

[17] M. Riebesell: "Raman-lidar zur Fernmessung von Wasserdampf- und Kohlendioxyd-Hhenprofilen in der Troposphre" Dissertation Univ. Hamburg, FB Physik, (1989)

[18] J. Cooney, K. Petri, and A. Salik: "Measurements of high resolution atmospheric water-vapor profiles by use of a solar blind Raman lidar" Appl. Opt. 24, 104-108 (1985)

[19] D. Renaut and R. Capitini: "Boundary-layer water vapor probing with a solar-blind Raman lidar: validations, meteorological observations, and prospects" J. Atmos. Oceanic Tech. 5, 585 - 601 (1988)

[20] W.B. Grant: "Differential absorption and Raman lidar for water vapor profile measurements: a review" Opt. Eng. 30, 40 - 48 (1991)

[21] R.M. Schotland: "Errors in the lidar measurement of atmospheric gases by differential absorption" J. Appl. Met. 13, 71-77 (1974)

[22] G. Megie: "Mesure de la pression et de la température atmosphériques par absorbtion différentielle lidar: influence de la largeur d'émission laser" Appl. Opt. 19, 34-43 (1980)

[23] C. L. Korb, C. Y. Weng: "A Theoretical Study of a Two-Wavelength Lidar Technique for the Measurement of Atmospheric Temperature Profiles" J. Appl. Met. 21, 1346-1355 (1982)

[24] V. E. Zuev, Yu. S. Makushkin, V. N. Marichev, A.A. Mitsel, V. V. Zuev: "Lidar differential absorption and scattering technique: theory" Appl. Opt. 22, 3733-3741 (1983)

[25] A. Ansmann: "Errors in ground based water-vaporDIAL measurements due to Doppler-broadened Rayleigh backscattering" Appl. Opt. 24, 3476-3480 (1985)

[26] C. Cahen, G. Megie: "A spectral limitation of the range resolved differential absorption lidar technique" J. Quant. Spectrosc. Radiat. Transfer 25, 151-157 (1981)

[27] A. Ansmann and J. Bösenberg: "Correction scheme for spectral broadening by Rayleigh scattering in differential absorption lidar measurements of water vapor in the troposphere" Appl. Opt. 26, 3026-3032 (1987)

[28] S. Ismail, E. V. Browell, G. Megie, P. Flamant, G. Grew: "Sensitivities in DIAL measurements from airborne and spaceborne platforms" 12th International Laser Radar Conference, 431-436 (1984)

[29] T. D. Wilkerson, G. Schwemmer, B. Gentry, L. P. Giver: "Intensities and N_2 collision-broadening coefficients measured for selected H_2O absorption lines between 715 and 732 nm" J. Quant. Spectrosc. Radiat. Transfer 22, 315-331 (1979)

[30] J. Bösenberg: "Measurements of the pressure shift of water vapor absorption lines by simultaneous photoacoustic spectroscopy" Appl. Opt. 24, 3531-3534 (1985)

[31] Yi-Yi Sun, Zhi-Ping Li, and J. Bösenberg: "Depolarization of polarized light caused by high altitude clouds. 1: Depolarization of lidar induced by cirrus" Appl. Optics 28, 3625 - 3632, 1989

[32] Yi-Yi Sun and Zhi-Ping Li: "Depolarization of polarized light caused by high altitude clouds. 2: Depolarization of lidar induced by water clouds" Appl. Optics 28, 3633 - 3638, 1989

[33] F. G. Fernald: "Analysis of atmospheric lidar observations: some comments" Appl. Opt. 23, 652 (1984)